Biotechnology Reports 25 (2020) e00418

Contents lists available at ScienceDirect

Biotechnology Reports

journal homepage: www.elsevier.com/locate/btre

Generation of biparatopic antibody through two-step targeting of fragment antibodies on antigen using SpyTag and SpyCatcher

Hiroki Akiba[a,b], Kensuke Takayanagi[b], Osamu Kusano-Arai[c], Hiroko Iwanari[c], Takao Hamakubo[c,d], Kouhei Tsumoto[a,b,e,*]

[a] Center for Drug Design Research, National Institutes of Biomedical Innovation, Health and Nutrition, 7-6-8 Saito-Asagi, Ibaraki, Osaka, 567-0085, Japan
[b] Department of Bioengineering, School of Engineering, The University of Tokyo, 7-3-1 Hongo, Bunkyo-ku, Tokyo, 113-8656, Japan
[c] Research Center for Advanced Science and Technology, The University of Tokyo, 4-6-1 Komaba, Meguro-ku, Tokyo, 153-8904, Japan
[d] Department of Protein-protein Interaction Research, Institute for Advanced Medical Sciences, Nippon Medical School, 1-396 Kosugimachi, Nakahara-ku, Kawasaki, 211-8533, Japan
[e] Medical Proteomics Laboratory, The Institute of Medical Science, The University of Tokyo, 4-6-1 Shirokanedai, Minato-ku, Tokyo, 108-8639, Japan

ARTICLE INFO

Article history:
Received 1 August 2019
Received in revised form 3 January 2020
Accepted 3 January 2020

Keywords:
Bio-layer interferometry
Biparatopic antibody
Bispecific antibody
Roundabout homolog 1 (Robo1)
Single-Chain Fv (scFv)
SpyCatcher
SpyTag

ABSTRACT

Biparatopic fragment antibodies can overcome deficiencies in avidity of conventional antibody fragments. Here, we describe a technology for generating biparatopic antibodies through two-step targeting using a pair of polypeptides, SpyTag and SpyCatcher, that spontaneously react to form a covalent bond between antibody fragments. In this method, two antibody fragments, each targeting different epitopes of the antigen, are fused to SpyTag and to SpyCatcher. When the two polypeptides are serially added to the antigen, their proximity on the antigen results in covalent bond formation and generation of a biparatopic antibody. We validated the system with purified recombinant antigen. Results in antigen-overexpressing cells were promising although further optimization will be required. Because this strategy results in high-affinity targeting with a bipartite molecule that has considerably lower molecular weight than an antibody, this technology is potentially useful for diverse applications.

1. Introduction

Antibodies are used in both therapeutic and diagnostic applications. Fab, single-chain Fv (scFv), single-domain antibodies (nanobodies), and small antibody-like scaffolds are attractive because of their reduced molecular weights, which enable tissue permeability, and lack of an unwanted Fc-mediated immune response [1]. However, antibody fragments are monovalent, and their interactions with antigen are often weak because of lack of avidity. One potential solution to this problem is to confer bivalency or multi-valency through fusion or conjugation [2–6]. Biparatopic antibodies (BpAbs), in which two antibody fragments or other binding units that recognize different epitopes are linked, are particularly promising [7–10]. We previously achieved effective targeting through bivalent molecules by linking two scFv units with a tag sequence (i.e., SpyTag or SpyCatcher) [11]. The previous experimental design achieved a BpAb with a total molecular weight of 60 kDa, which is far smaller than conventional IgG antibody. Therefore, strong binding activity with high avidity can be achieved under conditions of reduced molecular size.

Here, we propose a system to accomplish further reduction of the molecular weight through two-step targeting (Fig. 1A). First, each of two monoclonal antibodies (mAbs) or binding units that target different epitopes of the antigen is fused with one of a pair of covalent-bond-forming units designed to form a covalent bond between them. Second, the two tagged fragments are added serially to the antigen and thereby accumulate in sufficiently close proximity for spontaneous formation of a covalent bond between the two tags, thus generating a BpAb on the antigen. Because the resulting BpAb retains bivalency, high affinity should be achieved.

As an *in vitro* model to validate the proposed methodology, we used SpyTag and SpyCatcher. A covalent bond (isopeptide bond) spontaneously forms between SpyTag and SpyCatcher (Fig. 1B) [12–14]. This reaction is rapid, specific, and irreversible. The tags, SpyTag and SpyCatcher have been used in various applications including stabilization of macromolecular assemblies [15–22], antibody fusions [6,11,12,23–25], and stabilization of proteins via

Abbreviations: AntiHis-AF488, anti-penta·His Alexa Fluor 488 conjugate; BLI, bio-layer interferometry; BpAb, biparatopic antibody; B-STag, B5209B scFv fused with SpyTag; E-SCat, E2107 scFv fused with SpyCatcher; scFv, single-chain variable fragment.

* Corresponding author at: Center for Drug Design Research, National Institutes of Biomedical Innovation, Health and Nutrition, 7-6-8 Saito-Asagi, Ibaraki, Osaka, 567-0085, Japan.
E-mail address: tsumoto@bioeng.t.u-tokyo.ac.jp (K. Tsumoto).

https://doi.org/10.1016/j.btre.2020.e00418

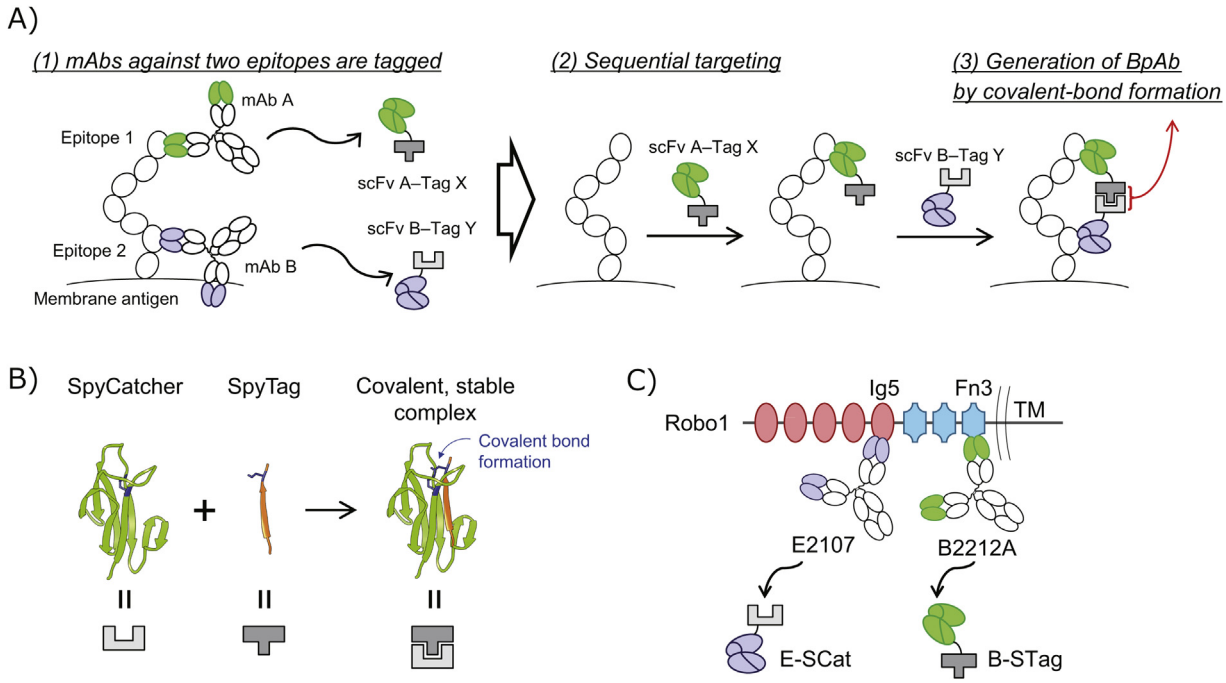

Fig. 1. A) Scheme of the sequential targeting protocol. First, two antibody fragments targeting different epitopes of an antigen molecule are each fused with one of a pair of covalent-bond-forming units. Second, the two fragments are serially added to the antigen. Third, a covalent bond spontaneously forms between the units, resulting in a biparatopic antibody (BpAb) fragment bound to antigen. B) The covalent-bond-forming units SpyCatcher and SpyTag. Ribbon diagrams produced from PDB ID 2X5P. C) Robo1 and the regions bound by the two mAbs used here. mAb E2107 binds to an Ig domain (red), and B2212A binds to an Fn domain (blue). The C-termini of scFvs produced from E2107 and B2212A were fused to SpyCatcher and SpyTag, respectively. TM, transmembrane domain. (For interpretation of the references to color in this figure legend, the reader is referred to the web version of this article.)

cyclization [26–28]. Building on the basic design of our previous work [11], we fused SpyTag and SpyCatcher to the C-termini of two different scFvs that target different domains of a cancer-related antigen, roundabout homolog 1 (Robo1) (Fig. 1C) [29]. These same Robo1 epitopes were targeted in our previous study [11]. The scFv generated from mAb B2212A, which binds the third fibronectin type III domain (Fn3) of Robo1 [30,31], was fused to SpyTag, and the scFv generated from mAb E2107, which binds the fifth immunoglobulin-like domain (Ig5), was fused with SpyCatcher. Each tag contains a C-terminal hexahistidine tag. The resulting B2212A-SpyTag (B-STag) and E2107-SpyCatcher (E-SCat) were expected to simultaneously bind to Robo1 resulting in covalent-bond formation between SpyTag and SpyCatcher and the formation of a BpAb with high affinity for Robo1.

2. Materials and methods

2.1. Antibody generation and selection

B2212A has been described previously [30]. E2107 was generated for use in this work. Briefly, human *Robo1* cDNA was amplified from Alexander cells and inserted into the pBlueBac 4.5-TOPO vector (Thermo Fisher Scientific). Recombinant baculovirus, collected from Sf9 culture media through centrifugation at 40,000 × *g* for 40 min, was resuspended in phosphate-buffered saline (PBS). Budded baculovirus expressing human Robo1 was used to immunize gp64 transgenic mice as previously described [29,32,33]. Isolated spleen cells were fused with myeloma cells as described [33]. Hybridomas were screened for secretion of antibody to Robo1. The reactivity of antibodies was assessed through cell-based ELISA and flow cytometry using the Chinese hamster ovary (CHO) cell line stably expressing human Robo1 (Robo1-CHO) [32]. The epitope of the selected antibody, E2107, was determined by competitive ELISA on Robo1-CHO with an antibody against the fifth immunoglobulin-like domain, B5209B [11,31,34].

2.2. Cloning of the variable region of E2107

Total RNA was extracted from 3×10^6 hybridoma cells by using 1 mL Trizol reagent (Invitrogen), and mRNA was purified from the total RNA by using Oligotex dT30 (Takara) according to the manufacturers' instructions. After removal of the transcripts encoding the kappa chain pseudogenes following the protocol described previously [35], the products were purified using the RNeasy Mini kit (Qiagen). cDNA was reverse-transcribed from the resulting mRNA. The genes encoding the variable regions of the

Table 1
Sequences of the linkers between the single-chain Fv (scFv) units and SpyTag or SpyCatcher.

	scFv C-termini (L-FR4[a])	Linker	SpyTag or SpyCatcher N-terminus[b]
B-STag	FGAGTKLELK	AAGGGGSGGGGS	AHIVMVDAYKPTK
E-SCat	FGSGKLEIK	SAGSSGSGS	VDTLSGLSSEQGQSGDMTIEED
E-SCat (−6 aa)	FGSGKLEIK	SAG	VDTLSGLSSEQGQSGDMTIEED
E-SCat (−17 aa)	FGSGKLEIK	SAG	GQSGDMTIEED

[a] Framework region 4 of the light chain variable region.
[b] For the SpyCatcher N-terminus sequence, the underlined Asp residue is the N-terminal amino acid observed in the crystal structure of SpyTag/SpyCatcher complex (PDB ID 4MLI).

heavy chain (VH) and light chain (VL) were amplified from the cDNA by using the Mouse Ig-Primer set (Novagen) and were cloned into the pUC118 vector using the Mighty Cloning Reagent Set (Blunt End) (Takara) according to the manufacturer's instructions. The DNA was sequenced, and the VH and VL amino acid sequences were identified using IgBLAST [36].

2.3. Preparation of proteins

The soluble recombinant extracellular domain of Robo1 (sRobo1) was prepared as previously described [30]. The gene encoding B2212A scFv was previously reported [30]. A gene designed to encode (from the N-terminus) the E2107 VH domain, a $(Gly_4Ser)_4$ linker, and the VL domain was optimized for expression in *Escherichia coli* and synthesized by Genewiz. Vectors encoding B-STag and E-SCat were constructed by inserting the genes encoding the scFv of B2212A and E2107 between the NcoI and SacII restriction sites of the pRA2 vectors encoding SpyTag- and SpyCatcher-fused scFvs described previously [11]. The vectors encoding E-SCat with different linker lengths were produced by an inverse PCR method using KOD-Plus-Neo Mutagenesis Kit (Toyobo). The linker sequences between the scFvs and SpyTag or SpyCatcher are listed in Table 1. Expression, refolding, and purification of B-STag and E-SCat, as well as preparation of the pre-formed BpAb (B-STag + E-SCat) followed previously described methods [11] except that the final purification by size-exclusion chromatography was conducted in 20 mM Tris-HCl, 500 mM NaCl, and 1 mM EDTA (pH 8.0) using a HiLoad 26/600 Superdex200 pg for E-SCat and a Superdex75 pg (GE Healthcare) for B-STag.

2.4. Bio-layer interferometry (BLI) for kinetic analysis

The Octet RED 384 System (ForteBio) was used. sRobo1 was immobilized on an AR2G chip as described previously [11]. The interaction was monitored in PBS containing 0.005% (v/v) Tween 20 (PBS-T) at 29 °C with a stirring rate of 1000 rpm. Kinetic analysis in multiple concentrations of antibody fragments and BpAb was conducted by analysis of two-fold dilution series of the polypeptides (B-STag, 0.313–5 nM; E-SCat, 1.25–20 nM; BpAb, 0.625–20 nM). During analysis of fragments (B-STag and E-SCat), both association and dissociation were monitored for 10 min. For the analysis of BpAb, association and dissociation were monitored for 20 min and 30 min, respectively, to account for slow dissociation rates.

2.5. BLI for two-step targeting

The immobilization and running conditions were as described in the previous section; targeting was monitored in three steps at 29 °C. After the baseline reached a plateau in PBS-T, 10 nM of the first antibody fragment (either E-SCat or B-STag) or an equivalent volume of PBS-T was added, and the sample was incubated for 10 min. The other antibody fragment (10 nM) or pre-formed BpAb (10 nM) or PBS-T was then added, and the sample was incubated for 10 min. Finally, dissociation was monitored for 10 min in PBS-T.

2.6. Reaction monitored through SDS-PAGE

The reaction was monitored by incubating 2 μM E-SCat and 2 μM B-STag in the presence or absence of 2 μM sRobo1 at 25 °C in PBS. Aliquots removed at the indicated time points were mixed with Laemmli sample buffer containing 710 mM 2-mercaptoethanol and heated at 95 °C for 5 min to denature proteins and quench the reaction. Samples from each time point were separated by SDS-PAGE, and the gel was stained with Coomassie brilliant blue (CBB) R-250. The intensity of CBB-stained bands was quantitated by the integration of the color density of the vertical section of the stained bands using ImageJ [37]. To standardize gels stained at different times, the average integrated values of sRobo1 were determined for each gel; relative band intensity was calculated from the integrated value of the band corresponding to the formed BpAb relative to the average sRobo1 value.

2.7. Flow cytometry

As a control, a CHO cell line stably expressing human roundabout homolog 4 (Robo4-CHO) was prepared by using the same protocol used to prepare Robo1-CHO cells [32]. For flow cytometry, we dissociated 3×10^5 Robo1-CHO and Robo4-CHO cells using 2.5 g/L trypsin containing 1 mM EDTA (Nacalai Tesque). Cells were washed with PBS containing 5% fetal bovine serum (Gibco); subsequent procedures were performed in this buffer. The cells were suspended in 2 nM of B-STag or buffer only, kept on ice for 30 min, washed twice, and suspended in 2 nM of E-SCat or buffer only. The cells were incubated on ice for 2 h, washed twice, suspended in Penta·His Alexa Fluor 488 conjugate (dilution, 1:200; Qiagen), and incubated on ice for 30 min. The cells were washed twice, filtered over a 40-μm cell strainer (Falcon, Corning), and analyzed in a flow cytometer (LSRFortessa, BD Biosciences) equipped with a high-throughput sampler using FACS Sheath Solution (BD Biosciences). Light scattering and fluorescence data were collected for 10,000 cells per condition. For fluorescence detection, a 488-nm-wavelength blue laser was used for excitation; emission was detected by using a standard filter at 530/30 nm. Data were analyzed by using FlowJo (version 10). Cell distribution plots were generated using a biexponential x-axis of the area of AlexaFluor488.

3. Results and discussion

3.1. Production of B-STag and E-SCat and their interactions with sRobo1

B-STag and E-SCat were expressed in the inclusion bodies of *E. coli* [11]. After protein refolding through multi-step dialysis as previously described [11], final purification was achieved through size-exclusion chromatography (Supporting Figure S1). The interaction between the antibody fragments and the soluble extracellular region of Robo1 (sRobo1) was analyzed using bio-layer interferometry (BLI) (Table 2 and Supporting Figure S2). B-STag interacted with immobilized sRobo1 with higher affinity (K_D = 426 pM) than did E-SCat (K_D = 5.97 nM) and had a seven-fold slower dissociation rate. Pre-formed BpAb (B-STag + E-SCat) that was produced by pre-incubation of the two fragments was also analyzed. As expected, BpAb had higher affinity for sRobo1 (K_D = 30.4 pM) than either fragment.

As the N-terminal region of SpyCatcher does not participate in the SpyTag/SpyCatcher pairing [13], we designed E-SCat proteins

Table 2
Kinetic parameters of the interaction of antibodies with sRobo1.[a]

	k_{on} ($\times 10^5$ $M^{-1}s^{-1}$)	k_{off} ($\times 10^{-4}$ s^{-1})	K_D (nM)
B-STag	6.6 ± 0.0	2.8 ± 0.0	0.43 ± 0.00
E-SCat	3.5 ± 0.1	21 ± 1	6.0 ± 0.1
B-STag + E-SCat (preformed)	2.1 ± 0.0	0.065 ± 0.002	0.030 ± 0.001
B-STag + E-SCat (−6 aa) (preformed)	2.3 ± 0.0	0.36 ± 0.00	0.16 ± 0.00
B-STag + E-SCat (−17 aa) (preformed)	2.4 ± 0.0	0.17 ± 0.00	0.072 ± 0.000

[a] Values are given as means ± S.E. after curve fitting of multi-cycle kinetics.

with shorter linkers (6 and 17 amino acids shorter) between scFv and SpyCatcher (Table 1). These shorter E-SCat constructs had slightly lower affinity for sRobo1 than the parent construct (Table 2 and Supporting Figure S2). The effect of the linker length was small, probably because of the proximity between Fn3 and Ig5 domains [38].

3.2. Two-step targeting monitored on BLI chips

Two-step targeting (Fig. 1A) was then monitored using BLI. Briefly, sRobo1 was immobilized on an amine-reactive sensor chip. The chip was dipped sequentially into solutions containing the first antibody fragment, the second antibody fragment, and the running buffer. When 10 nM B-STag was used as the first antibody and 10 nM E-SCat as the second, the bio-layer thickness reflecting the interaction was far larger than the sum of the thicknesses observed for either fragment individually (Fig. 2A, B). Furthermore, the response was maintained in the running buffer for 10 min, as it was with the pre-formed BpAb. This result indicated that the interaction between the two fragments, due to the spontaneous formation of a covalent bond between SpyTag and SpyCatcher, formed BpAb. Thus, the two-step targeting methodology was successful on a BLI sensor chip. The length of the linker in E-SCat did not alter efficiency of covalent bond formation under these conditions (Supporting Figure S3) as expected from the small difference in affinities of pre-formed BpAbs with varied linkers with sRobo1.

We also assessed our two-step targeting procedure using E-SCat as the first antibody fragment and B-STag as the second (Fig. 2A, C). In this case, the response was not enhanced as dramatically compared to the individual fragments alone as it was when B-STag was added to the antigen first. Due to the rapid dissociation of E-SCat from the antigen (Table 2), the two fragments were not simultaneously bound to the antigen and the amount of BpAb formed was reduced. Thus, slow dissociation of the first antibody fragment from the antigen is critical for two-step targeting.

3.3. Acceleration of covalent bond formation by two-step targeting

The experiment using BLI verified effectiveness of two-step targeting; however, it was still unclear if the simultaneous binding of the two fragments to the antigen accelerated formation of covalent bond or whether the sole interaction between SpyTag and SpyCatcher dominated BpAb formation. To discriminate between these two mechanisms, we used SDS-PAGE to analyze isopeptide bond formation in the presence and absence of sRobo1 as a function of time. In this experiment, B-STag, E-SCat, and sRobo1, each at a final concentration of 2 μM, were mixed. Over time, the intensities of bands at 30 kDa (B-STag) and 41 kDa (E-SCat) decreased, and a band at 71 kDa (BpAb) appeared (Fig. 3A).

As shown by quantification of band intensities, the amount of BpAb was higher at all time points in the presence of sRobo1 than in its absence (Fig. 3B). Moreover, the reaction proceeded more efficiently during the initial stage when sRobo1 was present. The gap between the intensities of sRobo1+ and sRobo1− was maintained after 5 min (Supporting Figure S4). The kinetics of isopeptide bond formation in the absence of sRobo1 were comparable to kinetics reported previously for bond formation between SpyCatcher and SpyTag (C-terminally tagged with maltose-binding protein) [12]. Therefore, the rate-limiting step in isopeptide bond formation in the absence of sRobo1 is the diffusion of B-STag and E-SCat. In the presence of sRobo1, B-STag and E-SCat are bound in close proximity, and this simultaneous binding enhances the covalent isopeptide bond formation. Given that the concentrations of the proteins in this experiment were 200-fold higher than the concentrations used in the BLI experiment, it was unlikely that BpAb formed in solution between B-STag and once-dissociated E-Scat played dominant roles in the BLI experiments (Fig. 2). Therefore, both antibody association to sRobo1 and isopeptide bond formation was necessary for effective targeting.

3.4. Two-step targeting in a whole-cell model

To analyze the utility of two-step targeting in live cells, B-STag, E-SCat, and anti-penta·His Alexa Fluor 488 conjugate (antiHis-AF488) were sequentially added to Robo1-CHO cells, and the cells were analyzed by flow cytometry. Incubation of Robo1-CHO cells with B-STag and antiHis-AF488 resulted in fluorescence enhancement reflecting the interaction of the secondary antibody; no fluorescence was observed when cells were incubated with E-SCat and the secondary antibody (Fig. 4). Sequential incubation of cells with B-STag, E-SCat, and antiHis-AF488 yielded a population of cells that fluoresced more strongly than others (Fig. 4 and Supporting Table 1). The mean fluorescence intensity of this population was nearly two-fold higher than the mean values of

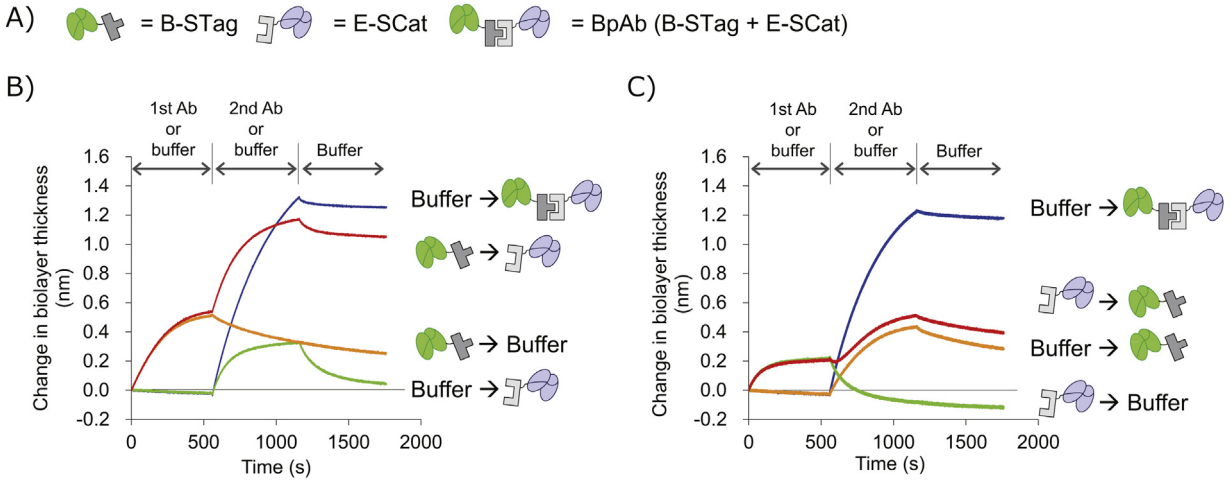

Fig. 2. A) Graphic representations of the antibody fragments. B, C) Changes in bio-layer thickness upon addition of the first antibody fragment, the second antibody fragment, and buffer. Responses were compared with one-step targeting of B-STag (orange), E-SCat (green), or pre-formed BpAb (blue) at 10 nM. In panel B, B-STag was as the first antibody fragment and E-SCat was the second. In panel C, E-SCat was first antibody fragment and B-STag was the second. (For interpretation of the references to color in this figure legend, the reader is referred to the web version of this article.)

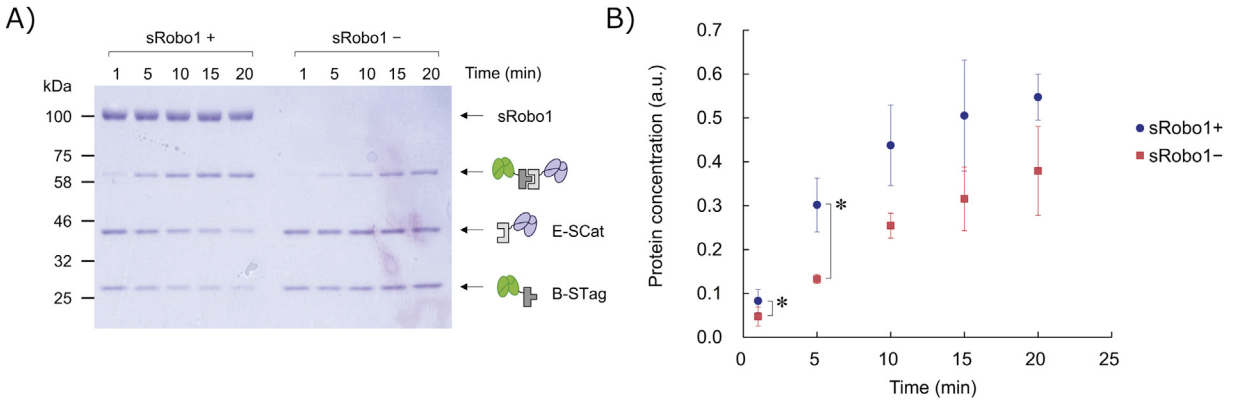

Fig. 3. A) Covalent bond formation between B-STag (2 μM) and E-SCat (2 μM) in the presence (left) or absence (right) of recombinant antigen sRobo1 (2 μM). Samples were analyzed at indicated times by SDS-PAGE. B) Intensity of the band corresponding to the BpAb at 71 kDa versus time in the presence of sRobo1 (blue) and in the absence of sRobo1 (red). Data are means ± S.D. of three independent experiments. $^*P < 0.05$. (For interpretation of the references to color in this figure legend, the reader is referred to the web version of this article.)

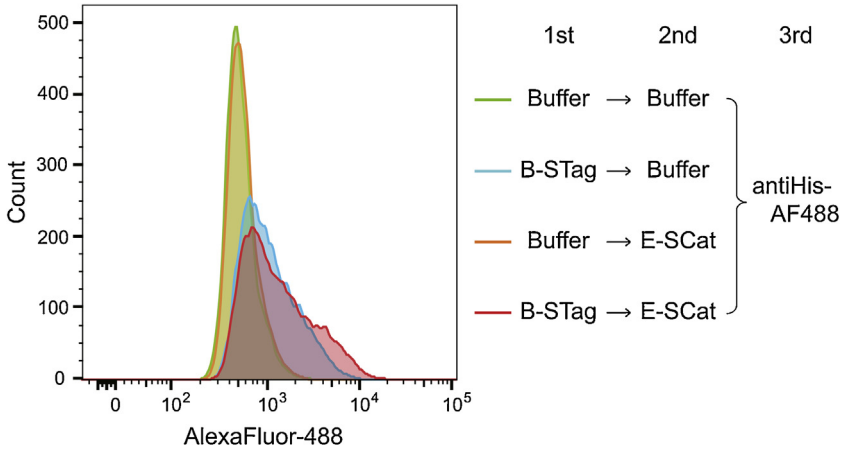

Fig. 4. Histograms of the areas of AlexaFluor 488 fluorescence. Robo1-CHO cells were incubated with antiHis-AF488 only (green); B-STag and antiHis-AF488 (cyan); E-SCat and antiHis-AF488 (orange); and B-STag, E-SCat, and antiHis-AF488 added sequentially (red). (For interpretation of the references to color in this figure legend, the reader is referred to the web version of this article.)

cells incubated only with B-STag and the secondary antibody. The increase in fluorescence was small and majority of cells were not likely observed with increased one, but the fluorescence exceeded the sum of the respective fluorescence enhancement by two fragments alone and thus suggested simultaneous, cooperative interaction between the two fragments. The specificity of the interaction was confirmed using Robo4-CHO cells (Supporting Figure S5). The difference in fluorescence between B-STag alone and sequential addition of B-STag and E-SCat when antigen was expressed on cells was smaller than the difference observed with recombinant protein (2 fold versus 4 fold).

This difference may be due to the cell surface environment that is not optimal for equal detection of the interaction of B-STag and E-SCat. Fluorescence did not enhance largely even when E-SCat fully interacted (Supporting Figure S6 and S7). This suggests that the His-tag of E-SCat is inaccessible to the secondary antibody. Additionally, there is heterogeneity in the expression level of Robo1 on the cells, and further optimization of experimental conditions will be required. Despite these drawbacks, the increase in the fluorescence upon two-step targeting compared use of a single fragment showed promise in the application of the methodology to the antigen expressed on the plasma membrane of a live cell when the cellular model is further optimized.

4. Conclusion

We have successfully built a model system to show BpAb formation by two-step targeting of a cancer-related antigen Robo1. Two fragments, SpyCatcher and SpyTag, which spontaneously form a covalent bond when in proximity, were used in the two-step targeting. The two-step targeting of antigen-expressing cells yielded only small population of cells with enhanced fluorescence relative to a single antigen binding fragment, but this result showed the potential of the system for antigen recognition on living cells. Using antibodies, their fragments, or fusion proteins in this type of two-step targeting will be useful in therapeutic and diagnostic applications as well as for biosensors.

Declaration of Competing Interest

None declared.

CRediT authorship contribution statement

Hiroki Akiba: Conceptualization, Investigation, Writing - original draft. **Kensuke Takayanagi:** Investigation. **Osamu Kusano-Arai:** Investigation, Writing - original draft. **Hiroko Iwanari:** Resources,

Validation. **Takao Hamakubo:** Conceptualization, Resources, Validation. **Kouhei Tsumoto:** Conceptualization, Validation, Writing - review & editing, Supervision.

Acknowledgements

We thank Reiko Satoh, Shinko Shimono, Chizuru Saruta, and Yumiko Yamagami for recombinant protein preparation. We also thank Dr. Noriko Komatsu for preparation of Robo1-CHO and Robo4-CHO cells, and we acknowledge technical assistance in flow cytometry from Dr. Tomoko Ise and Dr. Satoshi Nagata. This work was supported in part by AMED grant number JP18ak0101099, JSPS grant numbers JP25249115 and JP16H02420, Funding Program for World-leading Innovative R&D on Science and Technology (FIRST), and the Next-generation Technology Transfer Program from the Japan Science and Technology Agency (JST).

Appendix A. Supplementary data

Supplementary material related to this article can be found, in the online version, at doi:https://doi.org/10.1016/j.btre.2020.e00418.

References

[1] P. Holliger, P.J. Hudson, Engineered antibody fragments and the rise of single domains, Nat. Biotechnol. 23 (2005) 1126–1136, doi:http://dx.doi.org/10.1038/nbt1142.
[2] A. Todorovska, R.C. Roovers, O. Dolezal, A.A. Kortt, H.R. Hoogenboom, P.J. Hudson, Design and application of diabodies, triabodies and tetrabodies for cancer targeting, J. Immunol. Methods 248 (2001) 47–66, doi:http://dx.doi.org/10.1016/S0022-1759(00)00342-2.
[3] A. Plückthun, P. Pack, New protein engineering approaches to multivalent and bispecific antibody fragments, Immunotechnology. 3 (1997) 83–105, doi:http://dx.doi.org/10.1016/S1380-2933(97)00067-5.
[4] S.M. Cloutier, S. Couty, A. Terskikh, L. Marguerat, V. Crivelli, M. Pugnières, J.C. Mani, H.J. Leisinger, J.P. Mach, D. Deperthes, Streptabody, a high avidity molecule made by tetramerization of in vivo biotinylated, phage display-selected scFv fragments on streptavidin, Mol. Immunol. 37 (2001) 1067–1077, doi:http://dx.doi.org/10.1016/S0161-5890(01)00023-2.
[5] H. Albrecht, G.L. DeNardo, S.J. DeNardo, Monospecific bivalent scFv-SH: effects of linker length and location of an engineered cysteine on production, antigen binding activity and free SH accessibility, J. Immunol. Methods 310 (2006) 100–116, doi:http://dx.doi.org/10.1016/j.jim.2005.12.012.
[6] M.K. Alam, C. Gonzalez, W. Hill, A. El-Sayed, H. Fonge, K. Barreto, C.R. Geyer, Synthetic modular antibody construction by using the SpyTag/SpyCatcher protein-ligase system, ChemBioChem. 18 (2017) 2217–2221, doi:http://dx.doi.org/10.1002/cbic.201700411.
[7] F. Fleetwood, S. Klint, M. Hanze, E. Gunneriusson, F.Y. Frejd, S. Ståhl, J. Löfblom, Simultaneous targeting of two ligand-binding sites on VEGFR2 using biparatopic Affibody molecules results in dramatically improved affinity, Sci. Rep. 4 (2014) 7518, doi:http://dx.doi.org/10.1038/srep07518.
[8] M.E. Bradley, B. Dombrecht, J. Manini, J. Willis, D. Vlerick, S. De Taeye, K. Van den Heede, A. Roobrouck, E. Grot, T.C. Kent, T. Laeremans, S. Steffensen, G. Van Heeke, Z. Brown, S.J. Charlton, K.D. Cromie, Potent and Efficacious Inhibition of CXCR2 Signaling by Biparatopic Nanobodies Combining Two Distinct Modes of Action, Mol. Pharmacol. 87 (2015) 251–262, doi:http://dx.doi.org/10.1124/mol.114.094821.
[9] S. Jahnichen, C. Blanchetot, D. Maussang, M. Gonzalez-Pajuelo, K.Y. Chow, L. Bosch, S. De Vrieze, B. Serruys, H. Ulrichts, W. Vandevelde, M. Saunders, H.J. De Haard, D. Schols, R. Leurs, P. Vanlandschoot, T. Verrips, M.J. Smit, CXCR4 nanobodies (VHH-based single variable domains) potently inhibit chemotaxis and HIV-1 replication and mobilize stem cells, Proc. Natl. Acad. Sci. 107 (2010) 20565–20570, doi:http://dx.doi.org/10.1073/pnas.1012865107.
[10] G. Vauquelin, S.J. Charlton, Exploring avidity: understanding the potential gains in functional affinity and target residence time of bivalent and heterobivalent ligands, Br. J. Pharmacol. 168 (2013) 1771–1785, doi:http://dx.doi.org/10.1111/bph.12106.
[11] K. Yumura, H. Akiba, S. Nagatoishi, O. Kusano-Arai, H. Iwanari, T. Hamakubo, K. Tsumoto, Use of SpyTag/SpyCatcher to construct bispecific antibodies that target two epitopes of a single antigen, J. Biochem. 162 (2017) 203–210, doi:http://dx.doi.org/10.1093/jb/mvx023.
[12] B. Zakeri, J.O. Fierer, E. Celik, E.C. Chittock, U. Schwarz-Linek, V.T. Moy, M. Howarth, Peptide tag forming a rapid covalent bond to a protein, through engineering a bacterial adhesin, Proc. Natl. Acad. Sci. U. S. A. 109 (2012) E690–697, doi:http://dx.doi.org/10.1073/pnas.1115485109.
[13] L. Li, J.O. Fierer, T.A. Rapoport, M. Howarth, Structural analysis and optimization of the covalent association between SpyCatcher and a peptide tag, J. Mol. Biol. 426 (2014) 309–317, doi:http://dx.doi.org/10.1016/j.jmb.2013.10.021.
[14] S.C. Reddington, M. Howarth, Secrets of a covalent interaction for biomaterials and biotechnology: SpyTag and SpyCatcher, Curr. Opin. Chem. Biol. 29 (2015) 94–99, doi:http://dx.doi.org/10.1016/j.cbpa.2015.10.002.
[15] K.D. Brune, D.B. Leneghan, I.J. Brian, A.S. Ishizuka, M.F. Bachmann, S.J. Draper, S. Biswas, M. Howarth, Plug-and-Display: decoration of Virus-Like Particles via isopeptide bonds for modular immunization, Sci. Rep. 6 (2016) 19234, doi:http://dx.doi.org/10.1038/srep19234.
[16] F. Sun, W.-B. Zhang, A. Mahdavi, F.H. Arnold, D.A. Tirrell, Synthesis of bioactive protein hydrogels by genetically encoded SpyTag-SpyCatcher chemistry, Proc. Natl. Acad. Sci. 111 (2014) 11269–11274, doi:http://dx.doi.org/10.1073/pnas.1401291111.
[17] W. Ma, A. Saccardo, D. Roccatano, D. Aboagye-Mensah, M. Alkaseem, M. Jewkes, F. Di Nezza, M. Baron, M. Soloviev, E. Ferrari, Modular assembly of proteins on nanoparticles, Nat. Commun. 9 (2018) 1489, doi:http://dx.doi.org/10.1038/s41467-018-03931-4.
[18] G. Zhang, M.B. Quin, C. Schmidt-Dannert, Self-assembling protein scaffold system for easy in vitro coimmobilization of biocatalytic cascade enzymes, ACS Catal. 8 (2018) 5611–5620, doi:http://dx.doi.org/10.1021/acscatal.8b00986.
[19] K.D. Brune, M. Howarth, New routes and opportunities for modular construction of particulate vaccines: stick, click, and glue, Front. Immunol. 9 (2018) 1432, doi:http://dx.doi.org/10.3389/fimmu.2018.01432.
[20] M. Fairhead, G. Veggiani, M. Lever, J. Yan, D. Mesner, C.V. Robinson, O. Dushek, P.A. Van Der Merwe, M. Howarth, SpyAvidin hubs enable precise and ultrastable orthogonal nanoassembly, J. Am. Chem. Soc. 136 (2014) 12355–12363, doi:http://dx.doi.org/10.1021/ja505584f.
[21] L. Jia, K. Minamihata, H. Ichinose, K. Tsumoto, N. Kamiya, Polymeric SpyCatcher scaffold enables bioconjugation in a ratio-controllable manner, Biotechnol. J. 12 (2017)1700195, doi:http://dx.doi.org/10.1002/biot.201700195.
[22] S.K. Singh, S. Thrane, C.M. Janitzek, M.A. Nielsen, T.G. Theander, M. Theisen, A. Salanti, A.F. Sander, Improving the malaria transmission-blocking activity of a Plasmodium falciparum 48/45 based vaccine antigen by SpyTag/SpyCatcher mediated virus-like display, Vaccine. 35 (2017) 3726–3732, doi:http://dx.doi.org/10.1016/j.vaccine.2017.05.054.
[23] M.K. Alam, M. Brabant, R.S. Viswas, K. Barreto, H. Fonge, C. Ronald Geyer, A novel synthetic trivalent single chain variable fragment (tri-scFv) construction platform based on the SpyTag/SpyCatcher protein ligase system, BMC Biotechnol. 18 (2018) 55, doi:http://dx.doi.org/10.1186/s12896-018-0466-6.
[24] M.K. Alam, A. El-Sayed, K. Barreto, W. Bernhard, H. Fonge, C.R. Geyer, Site-specific fluorescent labeling of antibodies and diabodies using SpyTag/SpyCatcher system for in vivo optical imaging, Mol. Imaging Biol. 21 (2019) 54–66, doi:http://dx.doi.org/10.1007/s11307-018-1222-y.
[25] H. Kimura, R. Asano, N. Tsukamoto, W. Tsugawa, K. Sode, Convenient and universal fabrication method for antibody-enzyme complexes as sensing elements using the SpyCatcher/SpyTag system, Anal. Chem. 90 (2018) 14500–14506, doi:http://dx.doi.org/10.1021/acs.analchem.8b04344.
[26] X.W. Wang, W. Bin Zhang, Protein catenation enhances both the stability and activity of folded structural domains, Angew. Chem. Int. Ed. 56 (2017) 13985–13989, doi:http://dx.doi.org/10.1002/anie.201705194.
[27] M. Si, Q. Xu, L. Jiang, H. Huang, Spytag/spycatcher cyclization enhances the thermostability of firefly luciferase, PLoS One 11 (2016)e0162318, doi:http://dx.doi.org/10.1371/journal.pone.0162318.
[28] J. Wang, Y. Wang, X. Wang, D. Zhang, S. Wu, G. Zhang, Enhanced thermal stability of lichenase from Bacillus subtilis 168 by SpyTag/SpyCatcher-mediated spontaneous cyclization, Biotechnol. Biofuels 9 (2016) 79, doi:http://dx.doi.org/10.1186/s13068-016-0490-5.
[29] H. Ito, S.I. Funahashi, N. Yamauchi, J. Shibahara, Y. Midorikawa, S. Kawai, Y. Kinoshita, A. Watanabe, Y. Hippo, T. Ohtomo, H. Iwanari, A. Nakajima, M. Makuuchi, M. Fukayama, Y. Hirata, T. Hamakubo, T. Kodama, M. Tsuchiya, H. Aburatani, Identification of ROBO1 as a novel hepatocellular carcinoma antigen and a potential therapeutic and diagnostic target, Clin. Cancer Res. 12 (2006) 3257–3264, doi:http://dx.doi.org/10.1158/1078-0432.CCR-05-2787.
[30] T. Nakayama, E. Mizohata, T. Yamashita, S. Nagatoishi, M. Nakakido, H. Iwanari, Y. Mochizuki, Y. Kado, Y. Yokota, R. Satoh, K. Tsumoto, H. Fujitani, T. Kodama, T. Hamakubo, T. Inoue, Structural features of interfacial tyrosine residue in ROBO1 fibronectin domain-antibody complex: crystallographic, thermodynamic, and molecular dynamic analyses, Protein Sci. 24 (2015) 328–340, doi:http://dx.doi.org/10.1002/pro.2619.
[31] O. Kusano-Arai, R. Fukuda, W. Kamiya, H. Iwanari, T. Hamakubo, Kinetic exclusion assay of monoclonal antibody affinity to the membrane protein Roundabout 1 displayed on baculovirus, Anal. Biochem. 504 (2016) 41–49, doi:http://dx.doi.org/10.1016/j.ab.2016.04.004.
[32] K. Fujiwara, K. Koyama, K. Suga, M. Ikemura, Y. Saito, A. Hino, H. Iwanari, O. Kusano-Arai, K. Mitsui, H. Kasahara, M. Fukayama, T. Kodama, T. Hamakubo, T. Momose, A (90)Y-labelled anti-ROBO1 monoclonal antibody exhibits antitumour activity against hepatocellular carcinoma xenografts during ROBO1-targeted radioimmunotherapy, EJNMMI Res. 4 (2014) 29, doi:http://dx.doi.org/10.1186/s13550-014-0029-3.
[33] R. Saitoh, T. Ohtomo, Y. Yamada, N. Kamada, J. Nezu, N. Kimura, S. Funahashi, K. Furugaki, T. Yoshino, Y. Kawase, A. Kato, O. Ueda, K. Jishage, M. Suzuki, R. Fukuda, M. Arai, H. Iwanari, K. Takahashi, T. Sakihama, I. Ohizumi, T. Kodama, M. Tsuchiya, T. Hamakubo, Viral envelope protein gp64 transgenic mouse facilitates the generation of monoclonal antibodies against exogenous membrane proteins displayed on baculovirus, J. Immunol. Methods 322 (2007) 104–117, doi:http://dx.doi.org/10.1016/j.jim.2007.02.005.
[34] T. Yamashita, E. Mizohata, S. Nagatoishi, T. Watanabe, M. Nakakido, H. Iwanari, Y. Mochizuki, T. Nakayama, Y. Kado, Y. Yokota, H. Matsumura, T. Kawamura, T.

Kodama, T. Hamakubo, T. Inoue, H. Fujitani, K. Tsumoto, Affinity improvement of a cancer-targeted antibody through alanine-induced adjustment of antigen-antibody interface, Structure. 27 (2019) 519–527, doi:http://dx.doi.org/10.1016/j.str.2018.11.002 e5.

[35] C. Ostermeier, H. Michel, Improved cloning of antibody variable regions from hybridomas by an antisense-directed RNase H digestion of the P3-X63-Ag8.653 derived pseudogene mRNA, Nucleic Acids Res. 24 (1996) 1979–1980, doi:http://dx.doi.org/10.1093/nar/24.10.1979.

[36] J. Ye, N. Ma, T.L. Madden, J.M. Ostell, IgBLAST: an immunoglobulin variable domain sequence analysis tool, Nucleic Acids Res. 41 (2013) 34–40, doi:http://dx.doi.org/10.1093/nar/gkt382.

[37] C.A. Schneider, W.S. Rasband, K.W. Eliceiri, NIH Image to ImageJ: 25 years of image analysis, Nat. Methods 9 (2012) 671–675, doi:http://dx.doi.org/10.1038/nmeth.2089.

[38] N. Aleksandrova, I. Gutsche, E. Kandiah, S.V. Avilov, M.V. Petoukhov, E. Seiradake, A.A. McCarthy, Robo1 forms a compact dimer-of-Dimers assembly, Structure. 26 (2018) 320–328, doi:http://dx.doi.org/10.1016/j.str.2017.12.003 e4.